TAO, Vol. 8, No. 3, 345-354, September 1997

A Simulation Study of the Interaction Between a Fast Shock and the Heliopuase

L. C. Lee[1], B. R. Schmidt[2], H. J. Cai[2] and Y. C. Whang[3]

(Manuscript received 4 February 1997, in final form 9 May 1997)

ABSTRACT

In a one-dimensional hybrid simulation of a fast shock impinging on the heliopause(HP), it is found that two regions of increased plasma density are formed between the transmitted and reflected shocks. The region downstream of the shock, on the interstellar side of the heliopause, has typically twice the original plasma density. The density increase is dependent on the impinging shock speed. This region has a greatly enhanced ion temperature anisotropy $T_\perp / T_{//} \sim 100$ and a plasma beta $\beta \sim 0.1 - 1.0$, which may lead to the generation of ion cyclotron waves and mirror waves. The region downstream of the reflected shock, on the solar wind side of the heliopause, has typically a 25% increase in plasma density. The enhanced temperature anisotropy is $T_\perp / T_{//} \sim 1.2$, but the plasma beta is very high, $\beta \sim 20$, which may also lead to the generation of mirror waves and ion cyclotron waves.

(Key words: Fast shock, Heliopause, Shock interaction, Mirror wave, Ion cyclotron wave)

1. INTRODUCTION

Voyager spacecraft observations of very low frequency radio emissions(2-3.6 kHz) in the outer heliosphere[Kurth *et al.* 1984, Macek *et al.* 1991, Gurnett *et al.* 1993] have recently stirred interest in the termination shock, the outer solar wind, and the heliopause. The termination shock is a reverse fast shock where the solar wind jumps from supersonic to subsonic speed. The heliopause separates the high beta plasma of the solar wind from the low beta plasma of local interstellar space. Its existence was first proposed by Davis [1955]. Over the next decade, Voyager 1 and 2 and Pioneer 11 spacecraft may provide answers about the location, shape, and extent of the termination shock.

Gurnett *et al.* [1993] proposed that the fast leading shock of a global merged interaction region (**GMIR**) triggered the observed radio emissions at or near the heliopause, and then estimated the distance to the heliopause to be between 116 and 177 AU. A **GMIR** is an ex-

[1] Department of Earth Science, National Cheng Kung University, Taiwan, R.O.C.

[2] Geophysical Institute, University of Alaska, Fairbanks, AK99775

[3]Department of Mechanical Engineering, Catholic University of America, Washington, D. C.20064

panding spherical shell of high-speed solar wind plasma having a thickness of several AU and is believed to be formed from the merging of a series of solar flares [Burlaga *et al.*, 1993]. Whang and Burlaga [1994] and Whang *et al.* [1995] studied the interaction of an interplanetary **MHD** shock with the heliopause using an **MHD** formulation. They identified dense plasma regions which could account for the observed radio frequencies and also calculated possible locations for the termination shock and heliopause. Figure 1 shows the interaction of the 1991 **GMIR** shock with the termination shock and heliopause using the most likely locations for the termination shock and heliopause. The fast **GMIR** shock slows down after passing the termination shock and then crosses the subsonic outer heliosphere. Notice that the heliocentric distance to the termination shock increases after the passage of the fast **GMIR** shock. After contact with the heliopause, the fast **GMIR** shock splits into reflected and transmitted shocks. Whang *et al.* [1995] used stagnation conditions downstream of the termination shock to estimate the average solar parameters just inside the heliopause. The requirement of pressure balance across the heliopause puts constrains on interstellar value of plasma temperature, density, and magnetic field.

In this paper we present numerical simulation results of the interaction of a fast shock with the heliopause. The simulation uses a hybrid code that combines a particle treatment of the ions with a massless fluid treatment of the electrons. The heliopause is modeled as a tangential discontinuity (**TD**). First we discuss the simulation and the initial set-up. Next we present and explain the simulation results for a typical case. A large temperature anisotropy $T_\perp / T_{//} \cong 100$ is found downstream of the transmitted shock on the interstellar side of the heliopause. The effect of different shock speeds on the results is then examined by a parameter search. Finally we predict that the mirror and ion-cyclotron waves would be generated by anisotropic ion heating associated with the transmitted and reflected shocks.

Previous simulations of quasi-perpendicular shocks have shown that a substantial perpendicular heating does occur [Lee *et al.*, 1988; Schopke *et al.*, 1990]. The generation of ion cyclotron waves in a plasma with a significant pressure anisotropy has been studied by many authors [*e.g.*, Cornwall, 1965]. The generation of mirror waves by an anisotropic temperature has been studied by Hasagawa [1969], Price *et al.* [1986], Lee *et al.* [1988], and McKean *et al.* [1994]. Burgess and Schwarz [1988] and Wu *et al.* [1993] have simulated the interaction of a fast perpendicular shock with a tangential discontinuity in the solar wind. With a hybrid code, Mandt and Lee [1991] have simulated the interaction of a weak fast shock with a tangential discontinuity, representing Earth's magnetopause. In this paper, we simulate the interaction of a fast (**GMIR**) and the heliopause.

2. SIMULATION MODEL

The hybrid code used in our simulation is described by Swift and Lee [1983]. The code treats all variables as functions of one spatial component (x) and time. The ions are treated as particles and their dynamics are followed exactly (one spatial and all three velocity components), while the electrons are treated as a massless fluid of finite pressure. The initial electron to ion pressure ratio is set to 1. The displacement current is dropped from the equations since we are interested in low frequency waves. Charge neutrality is assumed in solving the field

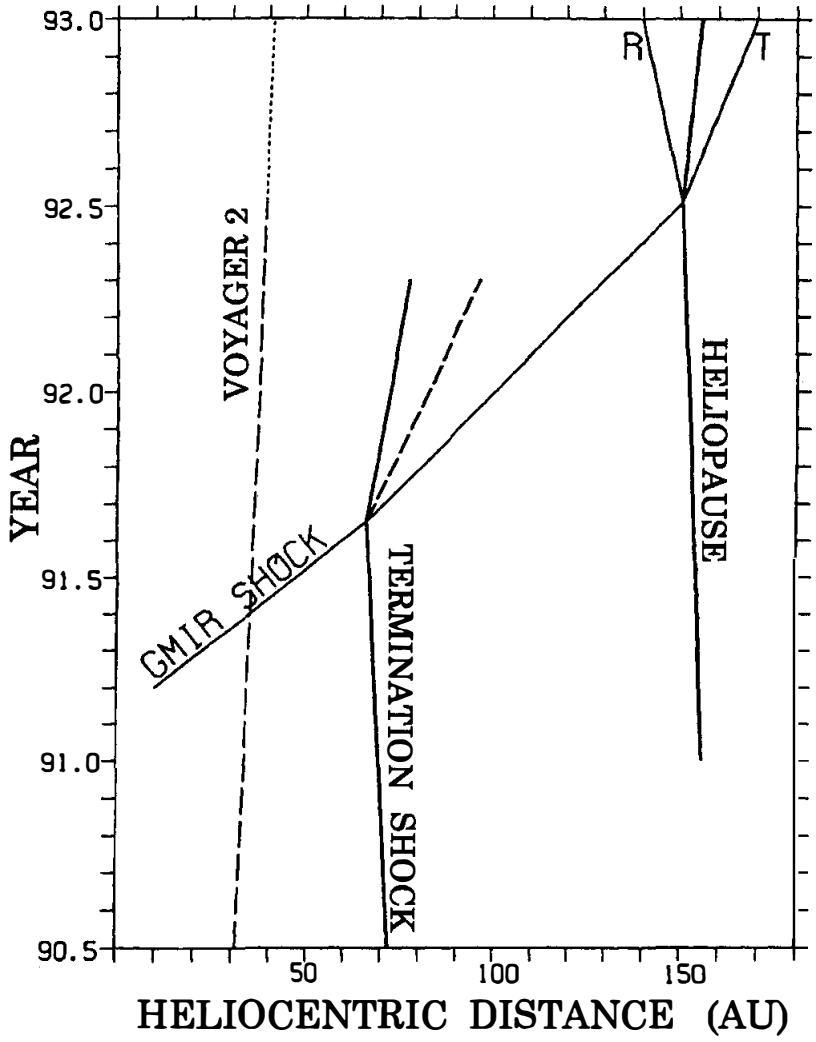

Fig. 1. A time vs. distance plot for a ~ 465 km/s 1991 GMIR. The leading edge of the fast GMIR shock penetrated through the temination shock at ~ 66 AU before it interacts with the heliopause at ~ 150 AU. The impingement of the fast GMIR shock at the heliopause produces a reflected shock (R) and a transmitted shock (T). The two regions bounded by these shocks have increased densities and the corresponding local plasma frequencies that are in tile 2-3.6 kHz range.

equations. We do not use anomalous resistivity in the code. The numerical procedure integrates two sets of equations, one for the vector field and one for the particles. The second-order differential equation for the field is implicitly integrated using a finite differencing method that is accurate to second order. The particle velocity equation is integrated every half time step using a leapfrog finite difference scheme. Buffer zones and inactive reservoirs are set up at each end of the simulation domain to ensure that the interruption of particle orbits does not introduce spurious boundary currents. Each buffer zone has a thickness of an ion gyrodiameter. This prevents the disruption of the ion orbits that pass into the buffer zone. This procedure is accurate as long as any perturbations coming from the ends of the simulation domain do not reach the central third, where we will examine the numerical results. This hybrid code has

been used successfully by others. Swift *et al.* [1983] studied rotational discontinuities. Lee *et al.* [1988] studied mirror wave generation downstream of a quasi-perpendicular shock. Mandt and Lee [1991] and Lin *et al.* [1996] simulated the interaction of dynamic pressure pulse and the magnetosheath.

Figure 2 illustrates the various plasma regions (using density) in the simulation domain. We model the heliopause (**HP**) as a **TD** which is centered in the simulation domain. The solar wind (region 1) and the downstream region of the fast **GMIR** shock (region 3) are on the right side of the **HP** and the interstellar plasma (region 2) is on the left. The resulting transmitted shock (**TS**) and reflected shock (**RS**) are the leading edges of region 4 and 5, respectively. The positive x-axis points toward the Sun along the shock normal and perpendicular to the magnetic field. The variation of plasma parameters across a discontinuity or shock is described by the Rankine-Hugoniot jump conditions. There are two conditions relating the plasma parameters across a **TD**: the normal net flow is zero and the total pressure (plasmas and magnetic) on either side remains equal. In our simulation, the plasmas on the two sides of **TD** are related by two ratios for density and magnetic field strength. The plasma and field parameter in region 3 are related to those in region 1 by the Rankine-Hugoniot conditions across the fast **GMIR** shock, which is determined by the upstream Alfven Mach number M_A of the shock and the plasma β.

The simulation is initialized with the fast **GMIR** shock just making contact with the **HP**, as in Fig. 2b. Thus there are initially only two regions in the simulation. First the interstellar plasma (region 2) is initialized in the code. Then the downstream plasma (region 3) is initialized using the plasma density ratio, magnetic field ratio across the **HP** and the upstream Alfven Mach number of the fast **GMIR** shock. The plasma parameters used in our simulation for the case in which the fast **GMIR** shock Alfven number $M_A = 8.5$ are listed in Table 1. Here $M_A = V_S / V_A$, where V_A is the Alfven speed in region 1 and V_S is the **GMIR** shock speed.

Plasma and field parameters are normalized by those in region 3, which is downstream of the **GMIR** shock. The simulation domain consists of 1601 grid points. The cell length is set to $\Delta x = 0.33\lambda_i$, where $\lambda_i = c/\omega_{pi}$, the ion plasma frequency $\omega_{pi} = (4\pi N_3 e^2 / m_i)^{1/2}$, m_i is the ion mass and N_3 is the plasma density in region 3. Simulation time is in units of $\Omega_3^{-1} = [eB_3 / m_i c]^{-1}$, the inverse ion gyrofrequency in region 3. A total of 54000 particles are initialized with a normalized density of 40 in region 2. The time step used is $t = 0.009\Omega_3^{-1}$.

3. SIMULATION RESULTS

Figure 3 shows several spatial profiles of plasma and field parameters at $t = 0$, $t = 9\ \Omega_3^{-1} = 140s$ and $t = 22\Omega_3^{-1} = 330s$, For this case ($M_A = 8.5$) we have $N_3 \cong 0.035cm^{-3}$, $B_3 \cong 0.69nT$, $\lambda_i = 1220km$ and $\Omega_3^{-1} = 15s$. Only the central third of the simulation domain is shown. The heliopause (**HP**), transmitted shock (**TS**), and reflected shock (**RS**) at $t = 22\Omega_3^{-1}$ are indicated on some of the profiles. Plots (d), (e), and (f) use a vertical logarithmic scale. The transmitted and reflected shocks are clearly visible, as is the motion of the tangential discontinuity. The shock impingement has produced two regions of increased plasma density and increased magnetic field strength on either side of the **HP**. In plot (c), two fast mode shock are clearly seen propagating away from the tangential discontinuity in opposite directions. Any widening of

Table 1. Plasma and field parameters.

	Region 1	Region 2	Region 3
B (nT)	.314	1.52	.687
N (cm^{-3})	.0159	.05	.0347
P (Pa)	8.98×10^{-13}	1.38×10^{-14}	3.86×10^{-12}
T (10^4 K)	410	2.0	800
V_X(km/s)	0	0	465
β	22.8	.015	20.6
V_A (km/s)	54.5	149	80.5
C_S (km/s)	184	12.9	258

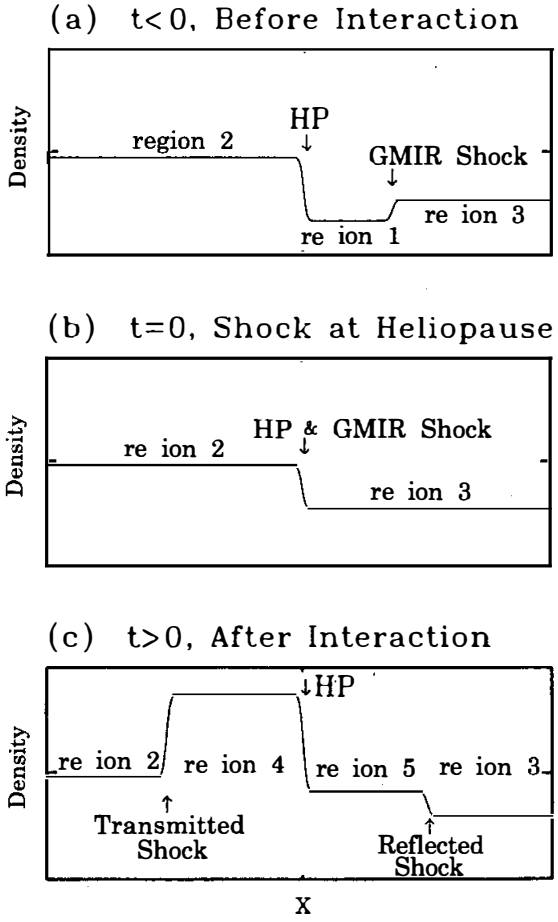

Fig. 2. The different plasma regions in the interaction of a fast shock with the heliopause (**HP**): (a) before the impingement, (b) at the moment of impingement, and (c) after the interaction, showing two additional regions behind the leading edges of the transmitted and reflected shocks.

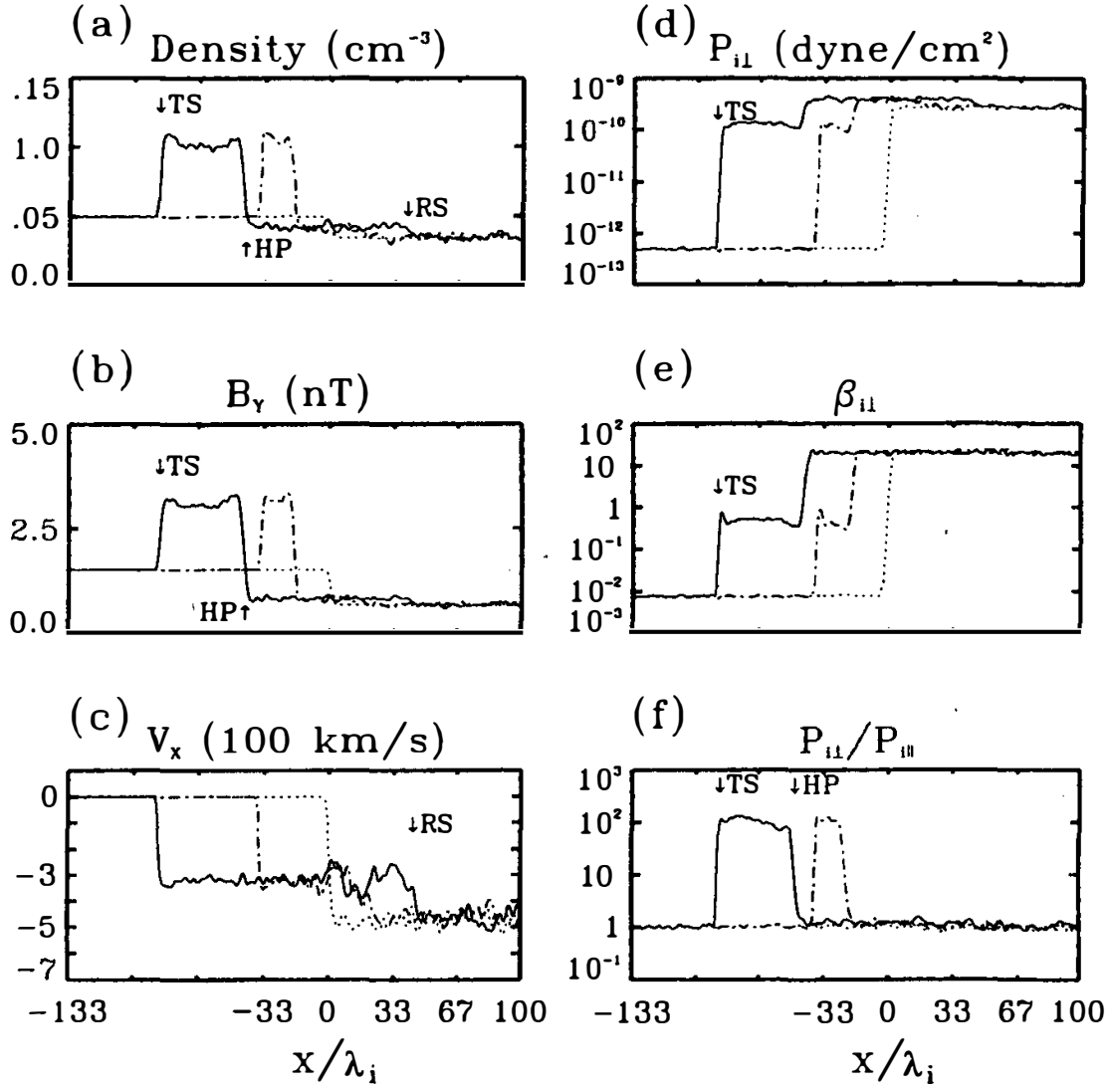

Fig. 3. Various spatial profiles of plasma and field parameters are shown at three different times: $t = 0$ (dot line), $t = 9\Omega_3^{-1}$(dot-dash line) and $t = 22\Omega_3^{-1}$(solid line), where Ω_3 is the ion gyrofrequency in region 3. The heliopause (**HP**), transmitted shock (**TS**), and reflected shock (**RS**) are indicated. Plot (a) shows the plasma density, (b) the magnetic field strength B_y, and (c) the velocity V_x. Plots (d), (e), and (f) are logarithmic plots. Plot (d) shows the perpendicular ion pressure $P_{i\perp}$ (e) the ion perpendicular plasma beta $\beta_{i\perp}$, and (f) the ion pressure anisotropy ratio $P_{i\perp} / P_{i//}$.

the tangential discontinuity's transition region is not yet discernible at $t = 22\Omega_3^{-1}$. The flow velocity in plot (c) is continuous across the **HP** and there is no net mass flux across the **HP**. In plot (f) it is seen that the temperature anisotropy is very large in region 4 since $P_\perp / P_{//} = T_\perp / T_{//} \cong 100$. In region 5 the temperature anisotropy is found to be 1.2 (average). These two values of anisotropy can be expected from estimates using the Rankine-Hugoniot equations [Mandt and Lee, 1991]. A large anisotropy can be generated in a low beta plasma even with a low shock Mach number, but not in a high beta plasma.

Figure 4 is a time series plot of the density profile for the case shown in Figure 3. The

heliopause (**HP**) is centered by using a frame moving to the left at ~275 km/s, slightly faster than the speed of the **HP**, which is convecting away from the sun. The transmitted shock (TS) and reflected shock (**RS**) fronts are clearly seen. From Table 1, the speed of a fast **GMIR** shock with M_A = 8.5 is 465 km/s in the solar frame. The speed of the transmitted and reflected shocks are ~350 km/s and ~170 km/s, respectively. The heliopause moves from its original location at ~180 km/s.

The effects of **GMIR** shock speed are presented in Figure 5. Plot (a) shows the temperature anisotropy plotted vs. the resultant perpendicular beta $\beta_\perp$ for both downstream regions of the transmitted and reflected shocks. The results from five different shock speeds are shown. For the transmitted shocks, the lowest $\beta_\perp$ is obtained for the case with **GMIR** shock speeds V_S = $7.0V_A$ which corresponds to the fast magnetosonic Mach number M_{MS} = 2.0. Here V_A is the Alfven speed in region 1, the solar wind plasma just inside of the heliopause. Plot (b) shows the plasma density ratio across the transmitted and reflected shocks. The reflected shock increases the density only slightly more than what the fast **GMIR** shock has already done. The downstream densities in regions 4 and 5 are obtained by averaging the density over the entire width of each of the two regions. The strength of a shock is best seen in the change of density. The transmitted shock is weaker than the original fast **GMIR** shock in all cases. For V_S = $8.5V_A$, the density change across the **GMIR** shock is ~2.18 and the density change across the transmitted shock is ~1.9.

4. GENERATION OF MIRROR WAVES AND ION CYCLOTRON WAVES

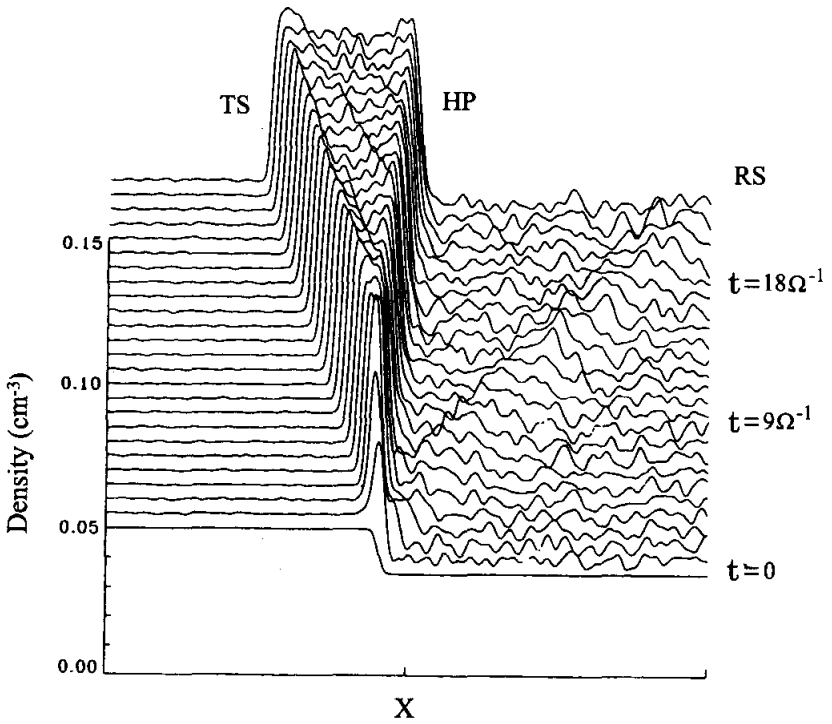

Fig. 4. Spatial profiles of density for the $V_S = 8.5V_A$ case in a time series. Each profile after the first is shifted along the x-axis to keep the heliopause (**HP**) centered. The transmitted (**TS**) and reflected shock (**RS**) fronts are clearly seen moving away from the **HP**.

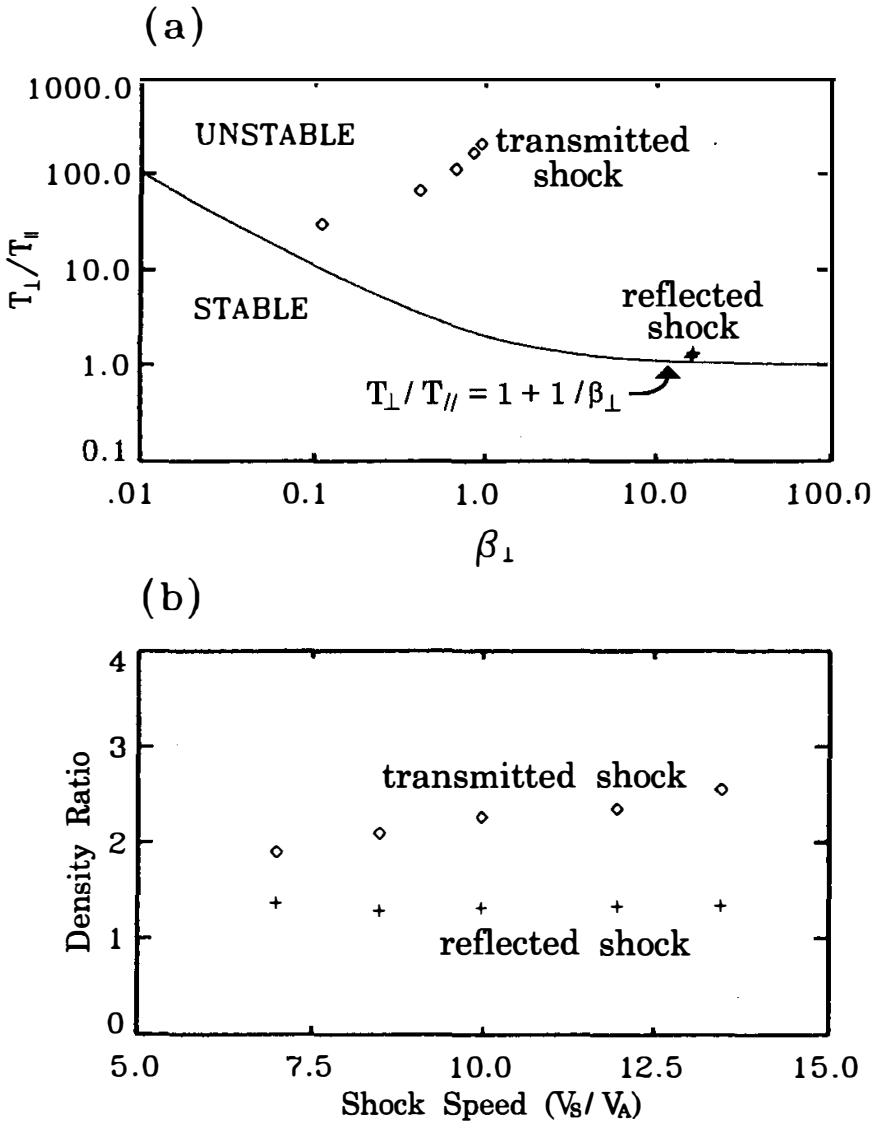

Fig. 5. (a) Temperature anisotropy ratios $T_\perp/T_{//}$ for different shock speeds are plotted vs. perpendicular plasma beta $\beta_\perp$. The stable and unstable regions are separated by the solid line, which is defined by $T_\perp/T_{//} = 1+1/\beta_\perp$. (b) Density ratios in regions 4 (transmitted shock) and 5 (reflected shock) plotted vs. Alfven mach number $M_A = V_S/V_A$ of the impinging fast shock.

The greatly enhanced temperature anisotropy in region 4 is from nonadiabatic ion heating of the low β interstellar plasma across the transmitted shock. The region 4 plasma can be unstable to mirror and ion cyclotron wave mode due to the large temperature anisotropy. The region 5 plasma has a much lower temperature anisotropy of ~1.2 but a higher plasma $\beta \sim 20$, and this region is also unstable to mirror waves and ion cyclotron waves.

The criterion for the mirror instability is $T_\perp/T_{//} > 1 + 1/\beta_\perp$, which is plotted in Fig. 5a. The stable and unstable regions are below and above the solid line, respectively. Fig. 5a shows that the plasmas in regions 4 and 5 for all cases simulated are unstable to mirror waves. The wave number k of the most unstable mode is typically $k \approx 0.5\rho_i^{-1}$ where ρ_i is the local ion

gyradius. The growth rate γ of the most unstable mirror waves can be estimated as $\gamma \approx 0.3\Omega_i$, in region 4, and $\gamma \approx 0.01\Omega_i$, in region 5, where Ω_i is the local ion cyclotron frequency [*e.g.*, Price *et al.*, 1986; Lee *et al.*, 1988].

The temperature anisotropy in regions 4 and 5 can also excite ion cyclotron waves. The growth of unstable ion cyclotron wave growth driven by a temperature anisotropy has been previously explored in hybrid simulations [*e.g.*, Price *et al.*, 1986; Mckean *et al.*, 1994]. The wavenumber of the most unstable mode is $k \approx 0.5\rho_i^{-1}$. The growth rate can be estimated as $\gamma \approx 0.1\Omega_i$. However, the presence of minor ions may reduce the growth rate of the ion cyclotron waves [Price at al., 1986].

In summary, we have used a hybrid code to simulate the interaction of the fast **GMIR** shock and the heliopause (**HP**). As a result of the interaction, a transmitted and reflected shock are present on the two sides of the heliopause. For the simulated parameters, the downstream region of the transmitted shock (interstellar side of **HP**) has an ion temperature anisotropy of $T_\perp / T_{//} \sim 100$ and a plasma beta $\beta \sim 0.1$ - 1.0. In the downstream region of the weaker reflected shock, $T_\perp / T_{//} \sim 1.2$ and $\beta \sim 20$. In both region, it is expected that both mirror waves and ion cyclotron waves are excited as a result of temperature anisotropy.

Acknowledgments This work was supported by a grant from National Science Council (NSC 86-2111-M-006-001-AP8) in Taiwan, ROC.

REFERENCES

Burgess, D. and S. J. Schwarz,1988: Colliding plasma structures: Current sheet and perpendicular shock. *J. Geophys. Res.*, **93**, 11327-11340.

Burlaga, L. F., F. S. McDonald and N. F. Ness,1993: Cosmic ray modulation and the distant heliospheric magnetic field: Voyager 1 and 2 observations from 1986 through 1989. *J. Geophys. Res.,* **98**, 1-12.

Cornwall, J. M.,1965: Cyclotron instabilities and electromagnetic emission in the ultra low frequency and very low frequency ranges. *J. Geophys. Res.,* **70**, 61-64.

Davis, L., Jr.,1955: It Interplanetary magnetic fields and cosmic rays. *Phys. Rev.,* **100**, 1440-1442.

Gurnett, D. A., W. S. Kurth, S. C. Allendorf and R. L. Poynter,1993: Radio emission from the heliopause triggered by an interplanetary shock. *Science,* **262**, 199-203.

Hasagawa, A.,1969: Drift mirror instability in the magnetosphere. *Phys. Fluids,* **12**, 2642-2644.

Kurth, W. S., D. A. Gurnett, F. L. Scarf and R. L. Poynter,1984: It Detection of radio emission at 3 kHz in the outer heliosphere. *Nature.* **312**, 27-31.

Lee L .C., C. S. Wu and X. W. Hu,1986: Increase of ion kinetic temperature across a collisionless shock: I. A new mechanism. *Geophys. Res. Lett.,* **13**, 209-212.

Lee, L. C., M. E. Mandt and C. S. Wu,1987: Increase of ion kinetic temperature across a collisionless shock: II. A simulation study. *J. Geophys. Res.*, **92**, 13438-13446.

Lee, L. C., C. P. Price, C. S. Wu and M.E. Mandt,1988: A study of mirror waves generated downstream of a quasi-perpendicular shock. *J. Geophys. Res.*, **93**, 247-250.

Lin, Y., L. C. Lee and M. Yan,1996: Generation of dynamic pressure pulses downstream of the bow shock by the variation of IMF orientation. *J. Geophys. Res.*, **101**, 479-493.

Mandt, M. E. and L. C. Lee,1991: Generation of Pc 1 waves by the ion temperature anisotropy associated with fast shocks caused by sudden impulse. *J. Geophys. Res.*,**96**, 17897-17901.

Macek, W. M., I. H. Cairns, W. S. Kurth and D. A. Gurnett,1991: Low-frequency radio emission in the outer heliosphere: constraints on emissions processes. *J. Geophys. Res.*, **96**, 3801-3806.

Mckean, M. E., D. Winske and S. P. Cary,1994: Two-dimensional simulations of ion anisotropy instabilities in the magnetosheath. *J. Geophys. Res.*, **99**, 11141-11153.

Price, C. P.,D. W. Swift and L. C. Lee,1986: Numerical simulation of nonoscilatory mirror waves at the Earth's magnetosheath. *J. Geophys. Res.*, **91**, 101-112.

Schopke, N., G. Paschmann, A. L. Brinca, C. W. Carlson and H. Luhr,1990: Ion thermalization in quasi-perpendicular shocks involoving reflected ions. *J. Geophys. Res.*, ***95, 6337-6352.***

Swift, D. W. and L. C. Lee,1983: Rotational discontinuities and the structure of the magnetopause. *J. Geophys. Res.*, **88**, 111-124.

Whang, Y. C., L. F. Burlaga,1994: Interaction of Global Merged Interaction Region Shock with the Heliopause and its Relation to the 2- and 3-kHz Radio Emissions. *J. Geophys. Res.*, **99**, 21457-21465.

Whang, Y. C., L. F. Burlaga and N. F. Ness,1995: Location of the termination shock and the heliosphere. *J. Geophys. Res.*, **100**, 17015-17023.

Wu. B. H., M. E. Mandt, L. C. Lee and J. K. Chao,1993: Magnetosphere response to solar wind dynamic pressure variation: interaction of interplanetary tangential discontinuities with the bow shock. *J. Geophys. Res.*, **98**, 21297-21311.s